

General Disclaimer

One or more of the Following Statements may affect this Document

- This document has been reproduced from the best copy furnished by the organizational source. It is being released in the interest of making available as much information as possible.
- This document may contain data, which exceeds the sheet parameters. It was furnished in this condition by the organizational source and is the best copy available.
- This document may contain tone-on-tone or color graphs, charts and/or pictures, which have been reproduced in black and white.
- This document is paginated as submitted by the original source.
- Portions of this document are not fully legible due to the historical nature of some of the material. However, it is the best reproduction available from the original submission.

NASA TM X- **65364**

CONVERSION OF ELECTROSTATIC PLASMA WAVE INTO ELECTROMAGNETIC WAVE—A NUMERICAL CALCULATION OF THE DISPERSION RELATION FOR ALL WAVE LENGTHS

HIROSHI OYA

SEPTEMBER 1970



———— GODDARD SPACE FLIGHT CENTER ————
GREENBELT, MARYLAND

FACILITY FORM 602	N70-42398	(ACCESSION NUMBER)		(THRU)
	33	(PAGES)		(CODE)
	TMX 65364	(NASA CR OR TMX OR AD NUMBER)		25
				(CATEGORY)

CONVERSION OF ELECTROSTATIC PLASMA WAVE INTO
ELECTROMAGNETIC WAVE - A NUMERICAL
CALCULATION OF THE DISPERSION
RELATION FOR ALL WAVE LENGTHS

by

Hiroshi Oya*

NASA, Goddard Space Flight Center
Greenbelt, Maryland

*NAS-NRC Resident Research Associate

ABSTRACT

The dispersion curves have been computed for a wide range of the wave length from the electromagnetic waves to the electrostatic waves in the case of the magnetoactive warm plasma with a Maxwellian velocity distribution function. The computation was carried out mainly for the perpendicular propagation mode. The upper hybrid resonance is the connection point of the electrostatic waves and the electromagnetic waves. The electrostatic waves not associated with the upper hybrid resonance are subjected to electron cyclotron damping when the wave length becomes long. Oblique propagation is allowed for the electrostatic waves in a frequency range from the plasma frequency to the upper hybrid resonance frequency in the long wave length region where Landau damping can be neglected and where the electrostatic mode smoothly connects to the electromagnetic X-mode. In a slightly inhomogeneous plasma the Bernstein mode electrostatic wave can escape by being converted into the O-mode electromagnetic wave; two reflections take place during this escape process. The frequency range of the escape coincides with the Cerenkov radiation of the electromagnetic waves, but these two mechanisms indicate clear contrast in its origin.

ABSTRACT

The dispersion curves have been computed for a wide range of the wave length from the electromagnetic waves to the electrostatic waves in the case of the magnetoactive warm plasma with a Maxwellian velocity distribution function. The computation was carried out mainly for the perpendicular propagation mode. The upper hybrid resonance is the connection point of the electrostatic waves and the electromagnetic waves. The electrostatic waves not associated with the upper hybrid resonance are subjected to electron cyclotron damping when the wave length becomes long. Oblique propagation is allowed for the electrostatic waves in a frequency range from the plasma frequency to the upper hybrid resonance frequency in the long wave length region where Landau damping can be neglected and where the electrostatic mode smoothly connects to the electromagnetic X-mode. In a slightly inhomogeneous plasma the Bernstein mode electrostatic wave can escape by being converted into the 0-mode electromagnetic wave; two reflections take place during this escape process. The frequency range of the escape coincides with the Cerenkov radiation of the electromagnetic waves, but these two mechanisms indicate clear contrast in its origin.

The electromagnetic Cerenkov radiation is produced interacting with the high energetic plasma beam with velocity range $100 v_{th} < v < 1000 v_{th}$ (for the nonrelativistic plasma), where v_{th} is the electron thermal velocity, while the origin of the electrostatic waves is in the interaction with the low energetic plasma beam.

1. INTRODUCTION

The Bernstein mode wave (Bernstein, 1958; Crawford, 1965) is the electrostatic approximation of the dispersion equation of plasma waves in a magnetoactive warm plasma for perpendicular propagation. In the extreme case of long wave lengths, the plasma waves exhibit the well known electromagnetic characteristics which were originally investigated by Appleton and Hartree (for a review, see Budden, 1961) for the case of a cold plasma. Shkarofsky (1968) and Dougherty (1969) have discussed the coupling region between the Bernstein waves and the electromagnetic waves in frequency ranges near the electron cyclotron harmonic frequencies.

In the present paper, the dispersion equation is investigated numerically to clarify the full nature of the plasma waves from the electrostatic to the electromagnetic modes over a wide frequency range. An escape mechanism of the electrostatic wave as a form of the electromagnetic wave is proposed relating to the upper hybrid frequency. The detailed discussion is carried out relating to the escape mechanism when the wave packet propagates through the slightly inhomogeneous plasma. The connection of the dispersion relation

for the oblique propagation in a wave length which is long enough to be free from the Landau damping effect has also been investigated relating to the transfer of the wave energy from the X-mode to the O-mode wave.

The extraordinary mode electromagnetic wave at the upper hybrid frequency has been observed in the laboratory plasma using a positive column of a weakly ionized hot-cathode arc discharge in helium with the magnetic field parallel to the column (Bekefi et al., 1962). The reception of the electromagnetic wave which propagates perpendicular to the magnetic field strongly suggests that the electrostatic oscillation can escape at the upper hybrid frequency. The present work provides a theoretical base for interpreting this evidence in terms of the escape mechanisms of the electrostatic wave as a form of the electromagnetic wave.

In the last part of this paper a brief discussion concerning the discrimination between the electromagnetic Cerenkov radiation and the electromagnetic wave which is produced as a reformation of the electrostatic wave propagating through an inhomogeneous medium is discussed because these two kinds of electromagnetic waves occur in the same frequency range between the plasma frequency and the upper hybrid frequency.

2. DISPERSION RELATIONS

The dispersion relation which has been summarized by Stix (1962) for the magnetoactive warm plasma can be derived from the wave equation

$$\vec{n} \times \vec{n} \times \vec{E} - (K) \vec{E} = 0 \quad (1)$$

where $\vec{n} = (c/\omega) \vec{k}$, \vec{k} is the wave vector, c is the velocity of light, and ω is the angular frequency. The matrix (K) is the equivalent dielectric tensor for the magnetoactive warm plasma with a Maxwellian velocity distribution function.

The elements of the tensor (K) have the form

$$(K) = \begin{bmatrix} K_{xx} & K_{xy} & K_{xz} \\ K_{yx} & K_{yy} & K_{yz} \\ K_{zx} & K_{zy} & K_{zz} \end{bmatrix}$$

where

$$\begin{aligned} K_{xx} &= 1 + i \sum_j \frac{\epsilon_j \pi_j^2}{\omega \Omega_j} \left(\frac{-\Omega_j \epsilon_j e^{-\lambda} \kappa T_{\perp j}}{m_j k_z} \right) \sum_{n=-\infty}^{\infty} \frac{n^2}{\lambda_j} I_n \langle \Theta \rangle_n \\ K_{xy} &= i \sum_j \frac{\epsilon_j \pi_j^2}{\omega \Omega_j} \left(\frac{-\Omega_j e^{-\lambda} \kappa T_{\perp j}}{m_j k_z} \right) \sum_{n=-\infty}^{\infty} i n (I_n - I'_n) \langle \Theta \rangle_n \\ K_{xz} &= i \sum_j \frac{\epsilon_j \pi_j^2}{\omega \Omega_j} \left(\frac{-\epsilon_j e^{-\lambda} \kappa T_{\perp j}}{m_j k_z} \right) \sum_{n=-\infty}^{\infty} \frac{n k_x}{\lambda_j} I_n \left\{ n \langle \Phi \rangle_n - \langle \Psi \rangle_n \right\} \end{aligned} \quad (2)$$

$$K_{yx} = i \sum_j \frac{\epsilon_j \pi_j^2}{\omega \Omega_j} \left(\frac{-\Omega_j e^{-\lambda} \kappa T_{\perp j}}{m_j k_z} \right) \sum_{n=-\infty}^{\infty} -in (I_n - I'_n) \langle \Theta \rangle_n$$

$$K_{yy} = 1 + i \sum_j \frac{\epsilon_j \pi_j^2}{\omega \Omega_j} \left(\frac{-\Omega_j e^{-\lambda}}{m_j k_z} \right) \sum_{n=-\infty}^{\infty} \left(\frac{n^2}{\lambda_j} I_n + 2\lambda I_n - 2\lambda I'_n \right) \langle \Theta \rangle_n$$

$$K_{yz} = i \sum_j \frac{\epsilon_j \pi_j^2}{\omega \Omega_j} \left(\frac{-e^{-\lambda} \kappa T_{\perp j}}{m_j k_z} \right) \sum_{n=-\infty}^{\infty} -ik_x (I_n - I'_n) (n \langle \Phi \rangle_n - \langle \Psi \rangle_n)$$

$$K_{zz} = 1 + i \sum_j \frac{\epsilon_j \pi_j^2}{\omega \Omega_j} \left(\frac{\Omega_j e^{-\lambda}}{k_z} \right) \sum_{n=-\infty}^{\infty} I_n \left\{ n \langle v_z \Phi \rangle_n - \langle v_z \Psi \rangle_n \right\}$$

and j indicates the different species of particle in the plasma. In the above expression $\epsilon_j = -1$ for electrons and $+1$ for ions; also π_j , Ω_j , $T_{\perp j}$, m_j , k_z , k_x , and v_z are the plasma frequency, the cyclotron frequency, the temperature corresponding to the velocity component perpendicular to the magnetic field, particle mass, the z and x components of the wave vector k , and the z component of the particle velocity v , respectively. The function I_n in eq. (2) is the modified Bessel function with argument λ_j ($\equiv k_x \kappa T / m_j$) and I'_n represents its first derivative. In the case of $T_{\perp} = T_{\parallel} = T$ and zero drift velocity the function in eq. (2), for a sufficiently high frequency range where only the electron motion is important, is re-written by

$$\langle \Theta \rangle_n = -2 \left(\frac{m}{2\kappa T} \right)^{3/2} F_0,$$

$$\langle v_z \Theta \rangle_n = 2i \left(\frac{m}{2\kappa T} \right) (1 + i \alpha_n F_0),$$

$$\langle \Phi \rangle_n = 0,$$

$$\langle v_z \Phi \rangle_n = 0,$$

$$\langle \Psi \rangle_n = 2i \left(\frac{m}{2\kappa T} \right) (1 + i \alpha_n F_0),$$

$$\langle v_z \Psi \rangle_n = \frac{2i}{k_z} \left(\frac{m}{2\kappa T} \right) (\omega + n\Omega) (1 + i \alpha_n F_0)$$

(3)

with

$$\alpha_n = \frac{\omega + n\Omega}{k_z} \left(\frac{m}{2\kappa T} \right)^{1/2}$$

and

$$F_0 = \sqrt{\pi} \frac{k_z}{|k_z|} \exp(-\alpha_n^2) + 2i \exp(-\alpha_n^2) \int_0^{\alpha_n} \exp \xi^2 d\xi,$$

where m , and ξ are the electron mass and a real variable, respectively. In the present case of nearly perpendicular propagation $\alpha_n \gg 1$; hence we can use the following approximate expression for F_0 :

$$F_0 = -\frac{i}{\alpha_n} \left(1 + \frac{1}{2\alpha_n^2} + \frac{3}{4\alpha_n^4} + \frac{15}{8} \frac{1}{\alpha_n^6} \right) \quad (4)$$

with an error less than 0.2% for $\alpha_n > 3$.

This relation is the dispersion equation of the well known Bernstein mode electrostatic waves.

In the extreme case of the long wave length, the elements of the dielectric tensor become

$$K_{xx} = K_{yy} \approx 1 - q_N^2 / (q^2 - 1),$$

$$K_{xy} \approx 0, \tag{9}$$

and $K_{zz} \approx 1 - q_N^2 / q^2$

where $q_N^2 = (\pi/\Omega)^2$

Rewriting $k_x c/\omega$ by n , eq. (7) reduces to the Appleton-Hartree relation for $\theta = 90^\circ$

$$n^2 = 1 - q_N^2 / (q^2 - 1)$$

and $\tag{10}$

$$n^2 = 1 - q_N^2 / q^2.$$

In the case of intermediate wavelengths all of the terms in eq. (7) must be retained. The next section presents numerical solutions of eq. (7) corresponding to this case.

3. NUMERICAL SOLUTIONS OF THE FULL WAVE DISPERSION RELATION

Computations have been carried out for $A = 2.97 \times 10^6$ ($T \approx 2000^\circ\text{K}$) and several values of the plasma parameter q_N ($= \pi/\Omega$) ranging from 0.2 to 4.5, as indicated in Figs. 1 to 4. The curves with $k_x R < 5 \times 10^{-3}$ are identical with the

dispersion curves of the electromagnetic waves except for the frequency range close to the cyclotron harmonics. The curves with $k_x R > 10^{-1}$ are identical with the dispersion curves of the Bernstein mode electrostatic waves where

$$R = \sqrt{\frac{\kappa T}{m\Omega^2}} .$$

In the intermediate wavelength region, i.e., between the extremes of pure electrostatic waves and pure electromagnetic waves, only waves described by the dispersion curves near the upper-hybrid frequency can persist; the waves corresponding to the other dispersion curves, which merge into the harmonics of the electron cyclotron frequency, are absorbed due to strong cyclotron damping. Although $k_z = 0$ is assumed in the present investigation, the actual propagation modes will include infinitely small k_z values rather than zero. This means that the wave is subjected to strong cyclotron damping effects when $\alpha_n < 3$ (see F_o in eq. (3)) which corresponds to the frequency range.

$$n\Omega - 3k_z \sqrt{\frac{2\kappa T}{m}} < \omega < n\Omega + 3k_z \sqrt{\frac{2\kappa T}{m}} . \quad (11)$$

Near the upper hybrid resonance, however, the wave is undamped and it is indicated (see Figs. 1 to 4) that the hybrid frequency is neither the resonance ($k \rightarrow \infty$, i.e., the wave length tends to zero) nor the cut off ($k \rightarrow 0$, i.e., the wave length tends to infinity), but provides a wave which creeps with relatively

low group velocity ($\partial\omega/\partial k_x$). When $q_N < 0.8$, the minimum value for the group velocity at the hybrid resonance frequency is less than $0.04 v_{th}$ where v_{th} is the electron thermal velocity which is defined by $R\Omega$. When $q_N > 1.6$, the minimum value for the group velocity is between 0.08 and $0.1v_{th}$. The magnetic field component gradually increases for wavelengths greater than about $200 \pi R$ which can be considered as the transition region between the electrostatic wave and the electromagnetic wave.

4. ESCAPE MECHANISMS OF THE ELECTROMAGNETIC WAVES FROM THE THERMAL PLASMA

a) Starting point

The above evidence that the electrostatic wave near the upper hybrid resonance continuously changes into an electromagnetic wave as the wave length increases, provides a theoretical foundation for the escape mechanism of Bernstein mode electrostatic wave energy as electromagnetic wave energy. These electrostatic waves may originate from instabilities in the plasma. In order to obtain the variation of the wave length, it is necessary to have an inhomogeneous plasma. To illustrate the escape mechanism we will consider a condition in which the direction of the electron density gradient makes a finite angle with respect to the superimposed magnetic field, and the wave starts propagating in the direction perpendicular to \vec{B} corresponding to decreasing q_N (see Fig. 5). Let us

consider a test wave packet that is constructed by a narrow band of sinusoidal waves with a center frequency ω_0 . These waves are indicated on the dispersion curve in Fig. 6 by A_d . Assume that this wave packet starts from the point A_m in the inhomogeneous plasma depicted in Fig. 5. When the wave is electrostatic, the propagation direction is strongly restricted by the direction of the constant magnetic field; since the component parallel to the magnetic field is subjected to thermal plasma damping the propagation direction is strongly localized in the direction perpendicular to the magnetic field.

b) The turn of electrostatic wave

Since we are assuming that the wave initially propagates in the direction of decreasing q_N , the dispersion curves will flatten out (see Figs 1-4) and the point on the curve corresponding to the center frequency of the wave packet will eventually merge with the point B_d in Fig. 6.

At this point the group velocity of the wave change from $\partial\omega/\partial k_x < 0$ to $\partial\omega/\partial k_x > 0$ and the test wave packet is reflected back towards the high q_N region. This turning point is shown by the point B_m in Fig. 5.

c) Passing through the upper hybrid resonance

After turning the wave packet propagates toward the region of the higher q_N where the dispersion curves build up

(see Figs 1-4) and the point on the curve correspond to the center frequency of the wave packet moves toward C_d in Fig. 6, where C_d marks the level of the upper hybrid resonance frequency. The group velocity of the wave around the upper hybrid resonance is not zero and the wave packet keeps progressing toward the high q_N region. When the wave length becomes larger than $200 \pi R$ (for example), the organized motion of the plasma generates a current which produces a significant magnetic field. Hence, the wave continuously changes from electrostatic to electromagnetic as the wave length increases while the packet propagates toward the high q_N region. For this case, the corresponding points are indicated as C_m and C_d in the model plasma in Fig. 5, and on the dispersion curves in Fig. 6, respectively.

d) Angle change and mode conversion

After passing through the region of the upper hybrid resonance frequency the ray direction of the test wave packet becomes more or less density dependent. This is partly because the wave propagation in an oblique direction with respect to the magnetic field is not severely damped in the long wave length region. In Fig. 7, the dispersion curves are plotted for oblique propagation with angles $\theta = 0^\circ, 15^\circ, 30^\circ, 45^\circ, 60^\circ, 75^\circ$ and 90° for $q_N = 1.6$. For oblique propagation, plasma thermal damping is very severe in the short wave length (large

k_x value) region. Thus the curves are plotted only for wave lengths longer than $26.7 \{R \cos \theta / (q + n)\}$. This criterion of the wave length limit is chosen to make α_n less than 3, in eq. (3), which makes the imaginary part of the function $i \alpha_n F_n$ less than 5×10^{-4} . The value k_x for a given constant frequency ω_o becomes smaller and the group velocity becomes larger, with increasing q_N , until the center frequency of the wave packet coincides with D_d (in Fig. 6). Then, the path of the wave packet propagation starts bending as indicated schematically in Fig. 5, after passing through the point C_m . When the wave packet arrives at the point D_m where $\omega_o = \pi$, all the dispersion curves for the different angles merge together as indicated by the point D_d in Fig. 6. At this point the part of the wave energy that can be transformed into the O-mode wave escapes from the plasma region from the point D_m as indicated in Fig. 5; the other part of the wave energy propagates in the plasma until it is reflected from the cut-off frequency ω_Z for the Z wave. After reflection the above mentioned mode conversion again takes place when the point D_d of Fig. 6 is encountered (E_m of Fig. 5). Part of this wave energy escapes as an O-mode wave and part of it experiences the reciprocal process of mode conversion, i.e., electromagnetic to electrostatic. This reciprocal process corresponds to the absorption of electromagnetic waves by a plasma (Budden

(1961), Denisov (1958) and Stix (1960)).

RELATION WITH CERENKOV RADIATION

As discussed in the previous section, electrostatic wave-energy can escape from an inhomogeneous plasma in the form of electromagnetic energy in the region where the wave frequency is between the local plasma frequency and the local upper hybrid frequency. This frequency range coincides with the frequency range of observed electromagnetic wave Cerenkov radiation which has been investigated by several workers (Jelly (1958), Kolomenskii (1956), Eidman (1962), Mckenzie (1964), Liemohn (1965), Seshadri and Tuan (1965), and Bauer and Stone (1968)).

The condition for Cerenkov radiation is

$$v \cos \theta = \omega/k \quad (12)$$

where v , and θ are the scalar velocity of the electron beam and the angle between the propagation vector \vec{k} and the electron beam velocity \vec{v} , respectively. The above mentioned authors let $\vec{k} \rightarrow \infty$ for the non relativistic beam where $v/c \rightarrow 0$. But as has been confirmed in the present paper, the electromagnetic approximation to the dispersion equation breaks down when $k \rightarrow \infty$. A proper solution requires the consideration of the full dispersion equation together with eq. (12). This equation is rewritten as

$$k R - \frac{q}{(v/v_{th}) \cos \theta} = 0 \quad (13)$$

The solution of eq. (13) can be obtained graphically as indicated in Fig. 8; the diagram indicates that Cerenkov radiation occurs for different wave lengths corresponding to different cross points of a given $(v/v_{th}) \cos \theta$ curve and the dispersion curves.

From this process we can see that the Cerenkov radiation associated with a high speed beam, $(v/v_{th}) \cos \theta > 100$, is electromagnetic in nature while the radiation associated with a beam of lower velocity is electrostatic in nature. For a very low beam velocity, $(v/v_{th}) \cos \theta < 10$, it is difficult for the Cerenkov radiation to escape in a wide frequency range between the local plasma frequency and the local upper hybrid frequency due to Landau damping. Thus, the only escape process for waves of short wavelength (shorter than the limiting value for the Landau damping) corresponds to perpendicular mode electrostatic wave which propagates through the inhomogeneous plasma.

CONCLUSION

Numerical calculations were carried out for the dispersion relation over a wide range of wavelengths from the electromagnetic waves to the electrostatic waves for a collisionless Maxwellian magnetoactive warm plasma. The computations were made mainly for the case of propagation

perpendicular to the superimposed magnetic field for several plasma conditions from $\pi/\Omega = 0.2$ to 4.5. The results indicate that the dispersion curves in the short wave length range (electrostatic wave range) merge into the harmonics of the electron cyclotron frequency when the wave length becomes longer except for the case of the upper hybrid resonance frequency. The merging of the dispersion curves into the harmonics of the electron-cyclotron frequency indicates that the electrostatic waves corresponding to these curves are subjected to strong cyclotron damping and thus cannot escape as electromagnetic waves. The upper hybrid frequency is neither the resonance frequency of the electromagnetic wave nor the cut-off frequency of the electrostatic wave, but designates the intermediate wave length region where the wave characteristics change gradually from electrostatic to electromagnetic with increasing wave length. When an electrostatic wave packet consisting of a narrow band of frequencies around the center frequency ω_0 starts to propagate through a slightly inhomogeneous plasma in the direction of decreasing π/Ω , the wave packet is reflected at the point where the group velocity changes from negative to positive, and propagates in the opposite direction. While passing through the upper hybrid resonance point,

$\omega_0 = \sqrt{\pi^2 + \Omega^2}$, the wave character gradually changes from electrostatic to electromagnetic. The special variation of the electron density near this point gradually changes the direction of the ray path. The wave normal direction also turns in the oblique direction with respect to the superposed magnetic field. Certain amounts of energy can be shared with the parallel component of the wave, i.e., the component with a wave normal directed parallel to the constant magnetic field. At the plasma frequency point ($\omega_0 = \pi$) part of the energy can be divided into the O-mode and part of it into the X-mode. The O-mode escapes from the plasma, whereas the X-mode continues to propagate in the plasma until it is reflected at the $\omega_0 = \omega_z$ cutoff point. When this reflected wave again encounters the $\omega_0 = \pi$ point, part of the wave energy escapes as an O-mode EM wave and part is converted to an electrostatic wave and is absorbed by the plasma.

The frequency range $\sqrt{\pi^2 + \Omega^2} > \omega > \Omega$ (for $\Omega > \pi$) or $\sqrt{\pi^2 + \Omega^2} > \omega > \pi$ (for $\pi > \Omega$), where the above described conversion of electrostatic wave energy to electromagnetic wave energy takes place, coincides with the frequency range of observed electromagnetic Cerenkov radiation. Thus this electromagnetic radiation may originate as electrostatic

Cerenkov radiation associated with a beam of low velocity electrons, ($v_{th} < v < 100 v_{th}$) in addition to the electromagnetic Cerenkov radiation associated with a high velocity beam ($v > 100 v_{th}$). It is also possible that plasma instabilities give rise to electrostatic waves which are then converted to electromagnetic waves; these waves may be erroneously attributed to Cerenkov radiation.

ACKNOWLEDGEMENT

I would like to express my sincere thanks to Drs. R.F. Benson, S.J. Bauer and R.G. Stone for their valuable discussions and encouragements to continue this work.

REFERENCES

- Bauer, S.J., and R.G. Stone (1968), Satellite observations of radio noise in the magnetosphere, *Nature* 218, No. 5147, 1145-1147.
- Bekefi, G., J.D. Coccoli, E.B. Hopper, and S.J. Buchsbaum (1962), Microwave emission and absorption at cyclotron harmonics of a warm plasma, *Phys. Rev. Letters* 9, No. 1, 6-9.
- Bernstein, I.B. (1958), Waves in a plasma in a magnetic field, *Phys. Rev.* 109, No. 1, 10-21.
- Budden, K.G. (1961), *Radio wave in the Ionosphere* (Cambridge Univ. Press, Cambridge).
- Crawford, F.W. (1965), Cyclotron harmonic waves in warm plasma, *Radio Science-J. Res. Natl. Bur. Std. USNC-URSI* 69D, No. 6, 789-805.
- Dougherty, J.P. (1969), Radiation from a dipole in magnetized plasma, *Plasma waves in space and in the laboratory*, (Editor: J.O. Thomas and B.J. Landmark, Edinburgh University press) 83-95.
- Denisov, N.G. (1958), Resonance absorption of electromagnetic waves by an inhomogeneous plasma, *Soviet Phys. JETP* 7, No. 2, 364-365.

- Eidman, V. Ya. (1962), Radiation of a plasma wave by a charge moving in a magnetoactive plasma, Soviet Phys. JETP 14, No. 6, 1401-1404.
- Jelly, J.V. (1958), Cerenkov Radiation (Pergamon Press, New York).
- Kolomenskii, A.A. (1956), Radiation from a plasma electron in uniform motion in a magnetic field, Soviet Phys. DOKLADY 1, No. 1, 133-136.
- Liemohn, H.B. (1965), Radiation from electron in a magnetoplasma, Radio Science-J. Res. Natl. Bur. Std. USNC-URSI 69D, No. 5, 741-766.
- McKenzie, J.F. (1964), Electromagnetic Radiation generated by a current source in an anisotropic medium, Proc. Phys. Soc. 84, Pt. 2, No. 538, 269-279.
- Seshadri, S.R., and H.S. Tuan (1965), Radiation from a uniformly moving charge in an anisotropic two component plasma, Radio Science-J. Res. Natl. Bur. Std. USNC-URSI 69D, No. 5, 767-783.
- Shkarovsky, I.P. (1968), Higher order cyclotron harmonic resonances and observation in the laboratory and in the ionosphere, J. Geophys. Res. 73, No. 15, 4859-4867.

Stix, T.H. (1960), Absorption of plasma waves, Phys. Fluids 3,

No. 1, 19-32.

Stix, T.H. (1962), The theory of plasma waves, (McGraw-Hill

Book, New York).

FIGURE CAPTIONS

- Figure 1. $\omega/\Omega - kR$ diagrams (dispersion curves) of the plasma waves which propagate in the direction perpendicular to the constant magnetic field for $q_N = 0.2$ and 0.8 ; k is equal to k_x in the text.
- Figure 2. Same as Fig. 1 with $q_N = 2.0$ and 2.5 .
- Figure 3. Same as Fig. 1 with $q_N = 3.0$ and 3.5 .
- Figure 4. Same as Fig. 1 with $q_N = 4.0$ and 4.5 .
- Figure 5. Change of the relative position of the frequency range, corresponding to the test wave packet, from A_d to E_d while the wave packet progresses through an inhomogeneous plasma.
- Figure 6. Schematic illustration of the path of the wave packet propagation through the inhomogeneous plasma in which the gradient of plasma density ∇n makes an arbitrary angle with respect to the magnetic field \vec{B}_0 ; the points from A_m to E_m are discussed in the text corresponding to A_d to E_d of Figure 5.

Figure 7. $\omega/\Omega - kR$ diagrams for propagation in the direction with angle 0° to 90° with respect to the magnetic field; Dotted area between $kR = 9 \times 10^{-2}$ to 4×10^{-1} , where $k = k_x/\sin \theta$, indicates that the waves propagating in oblique directions are subjected to damping.

Figure 8. Graphical solution of equation 13 relating the wavelength of Cerenkov radiation to the particle velocity v ; the solutions are indicated by the cross points between the solid and dashed curves corresponding to the given value of v and θ ; θ dependency of the solid curves is same as Fig. 7.

Figure 1

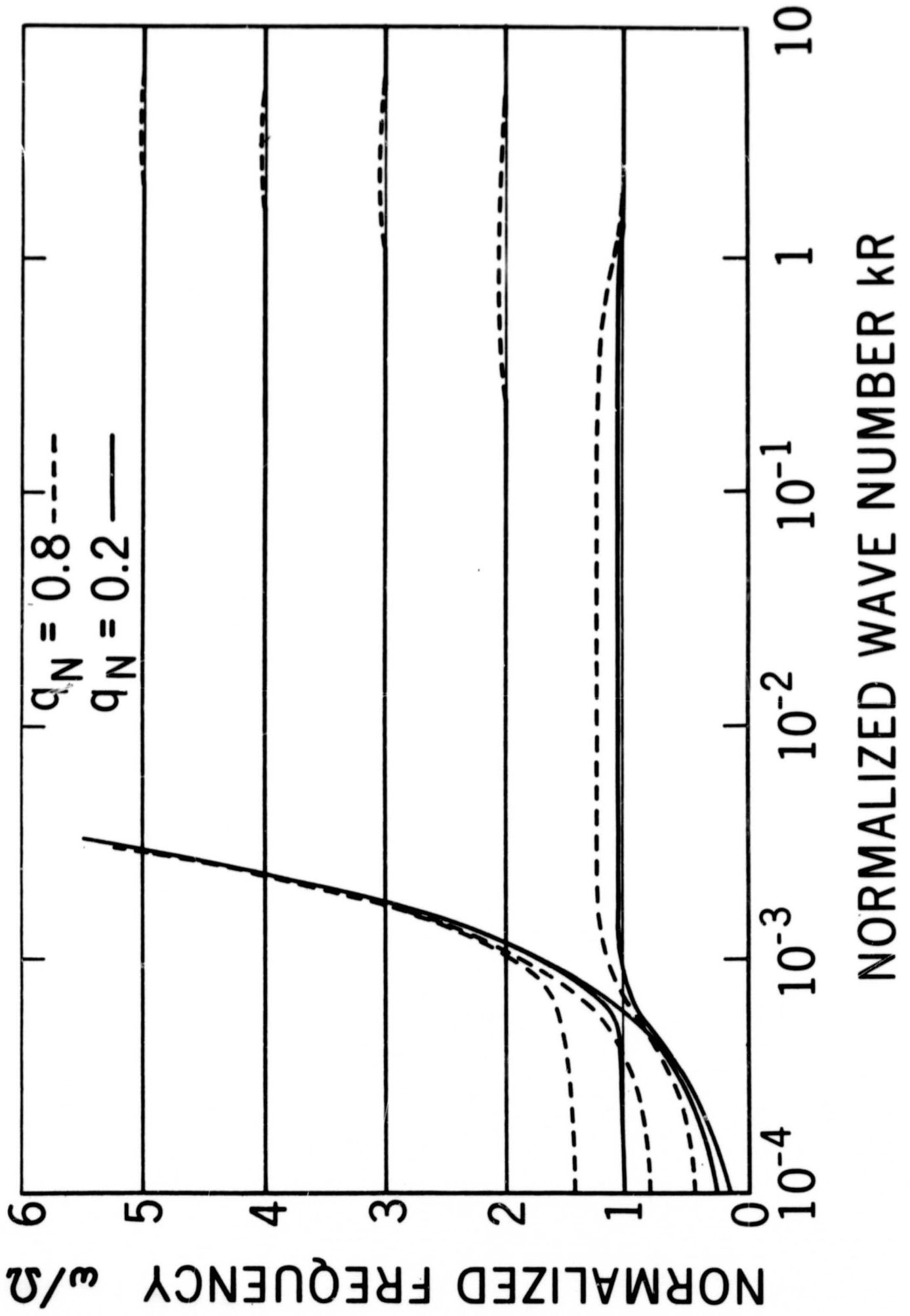


Figure 2

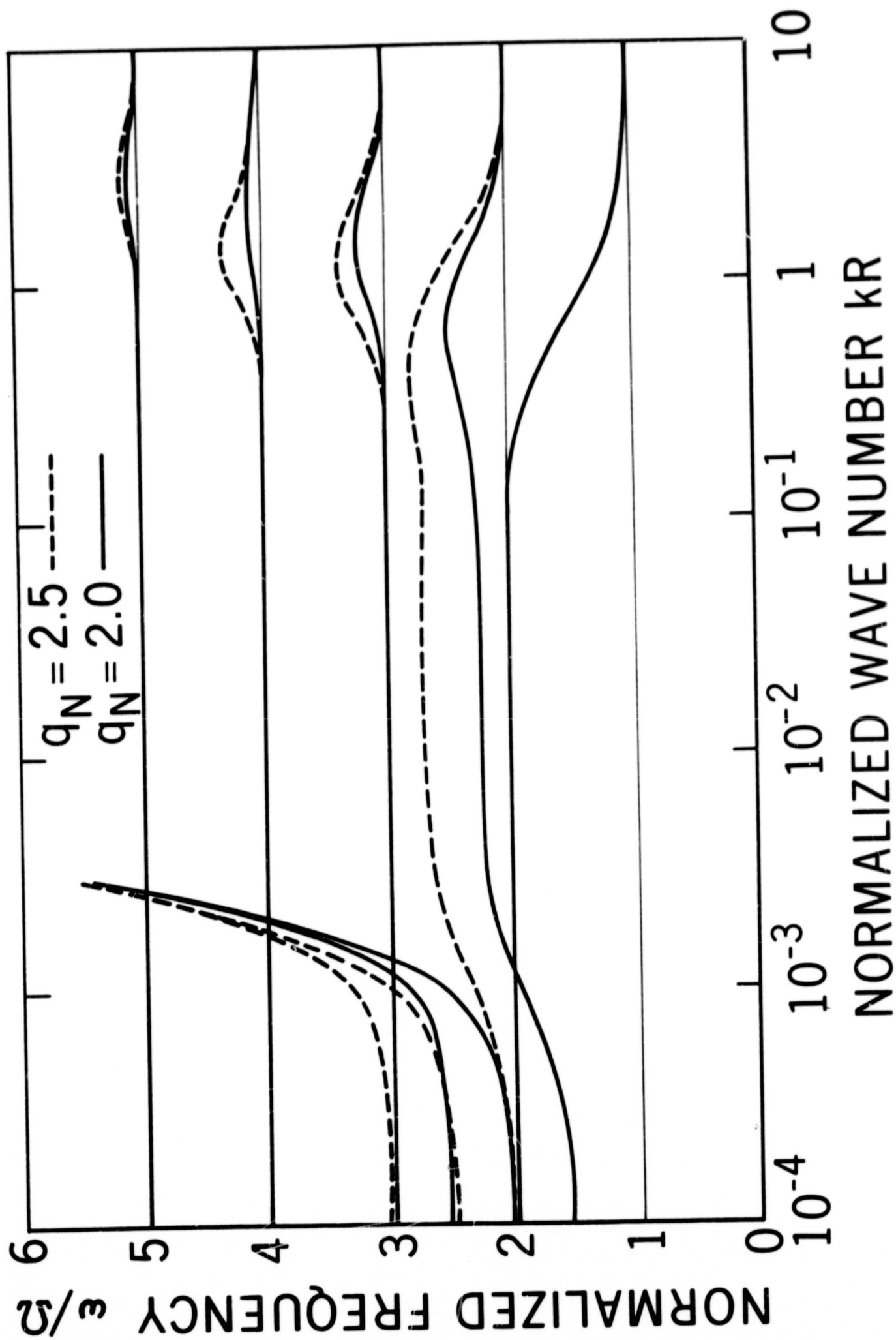


Figure 3

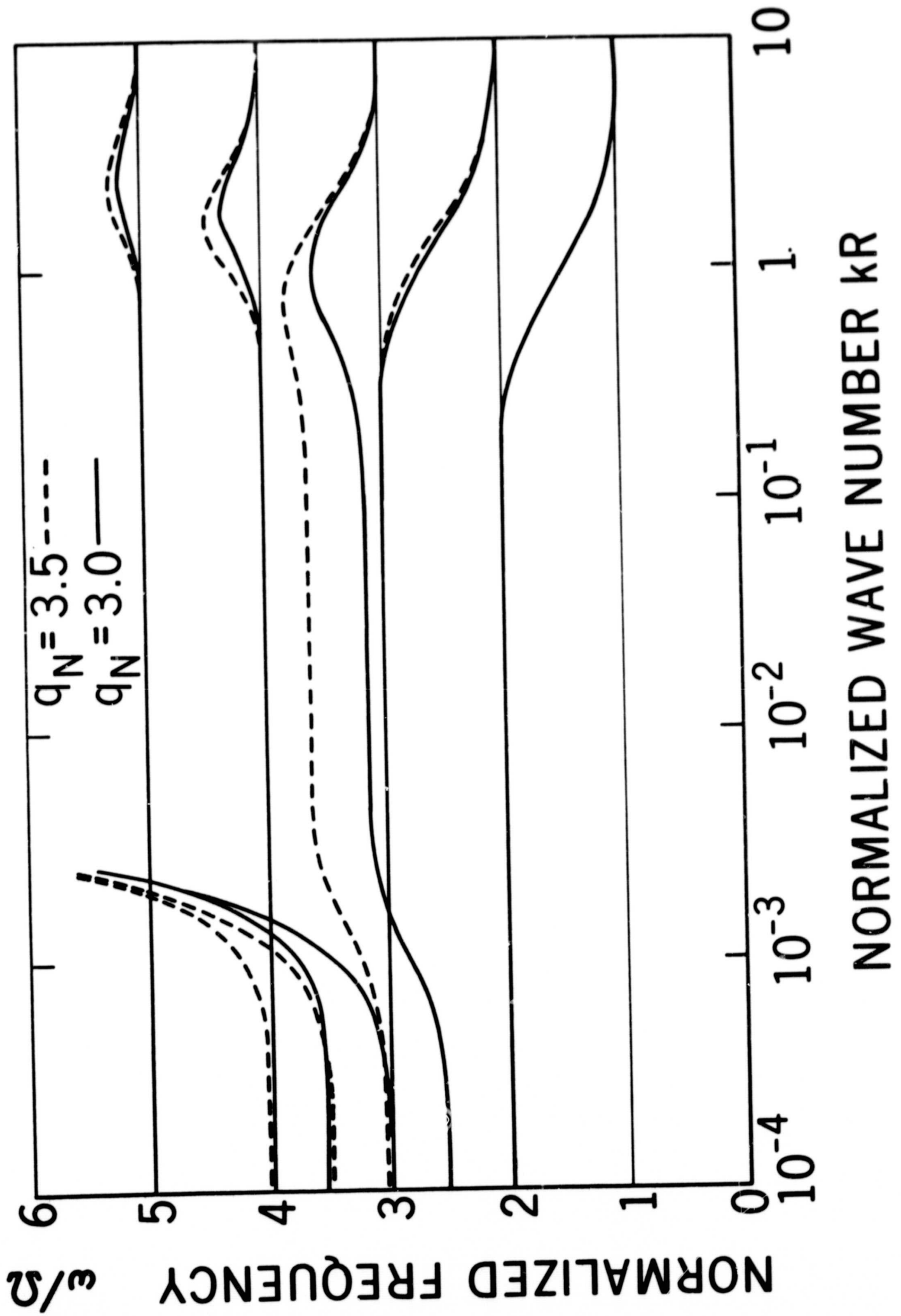


Figure 4

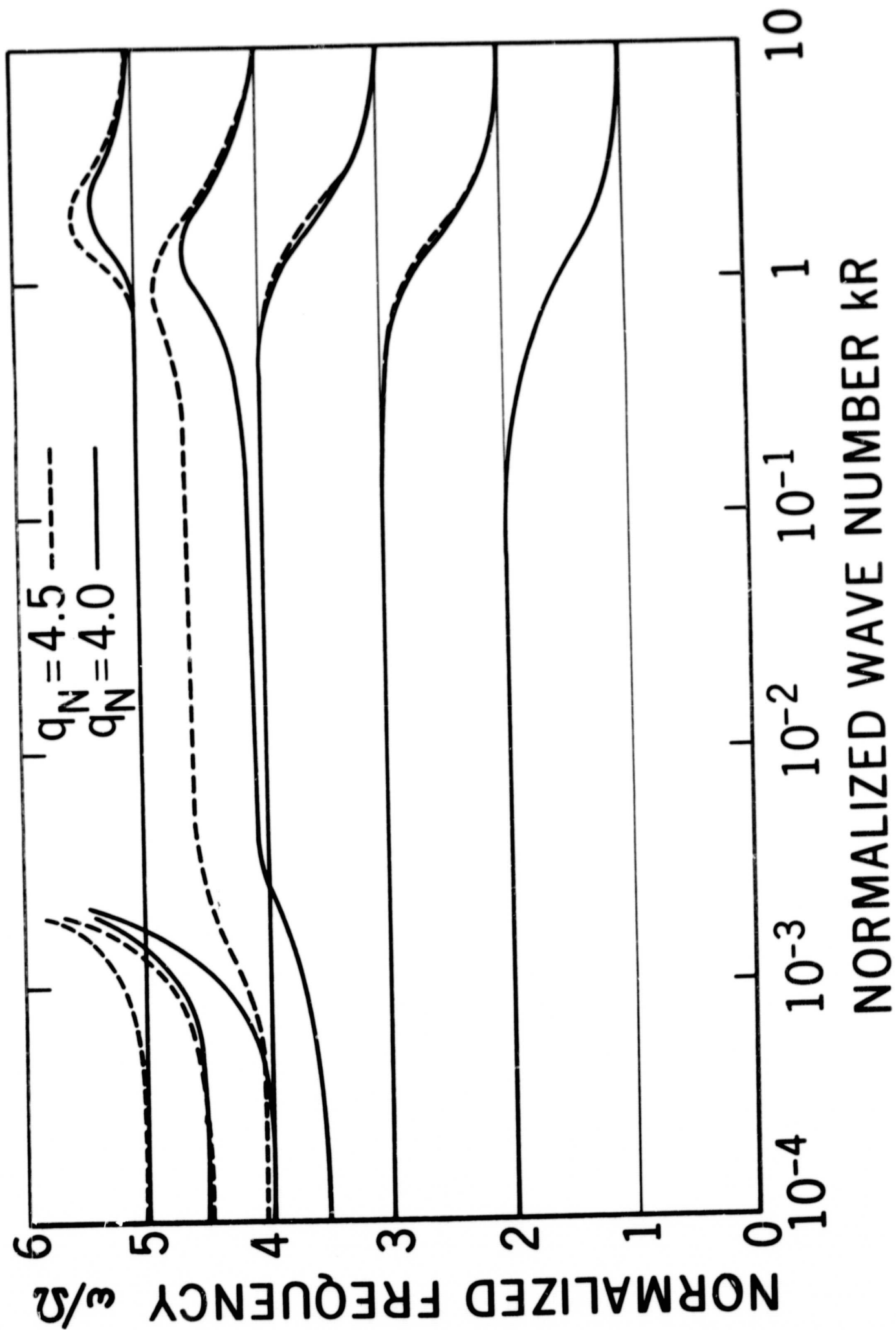


Figure 5

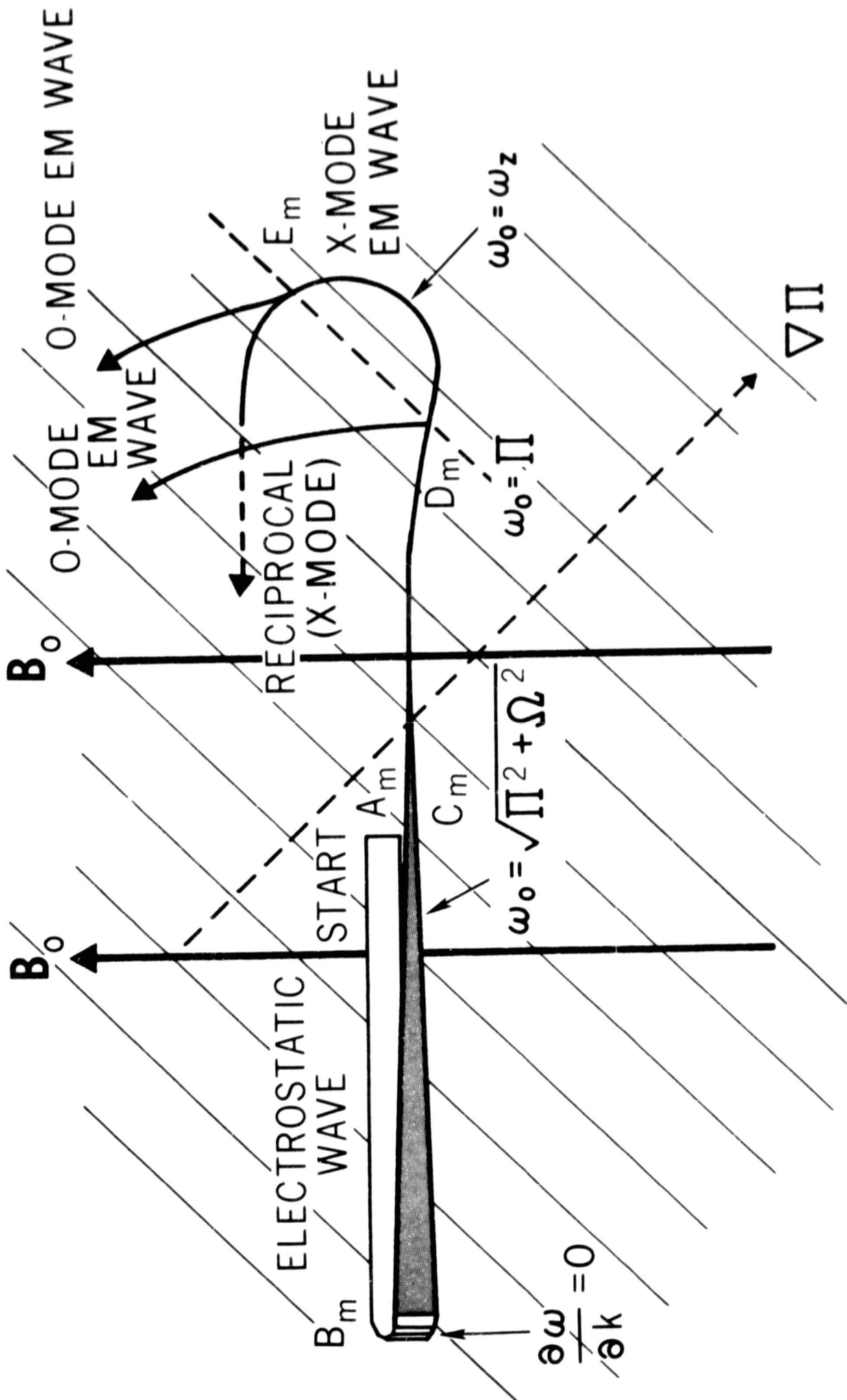


Figure 6

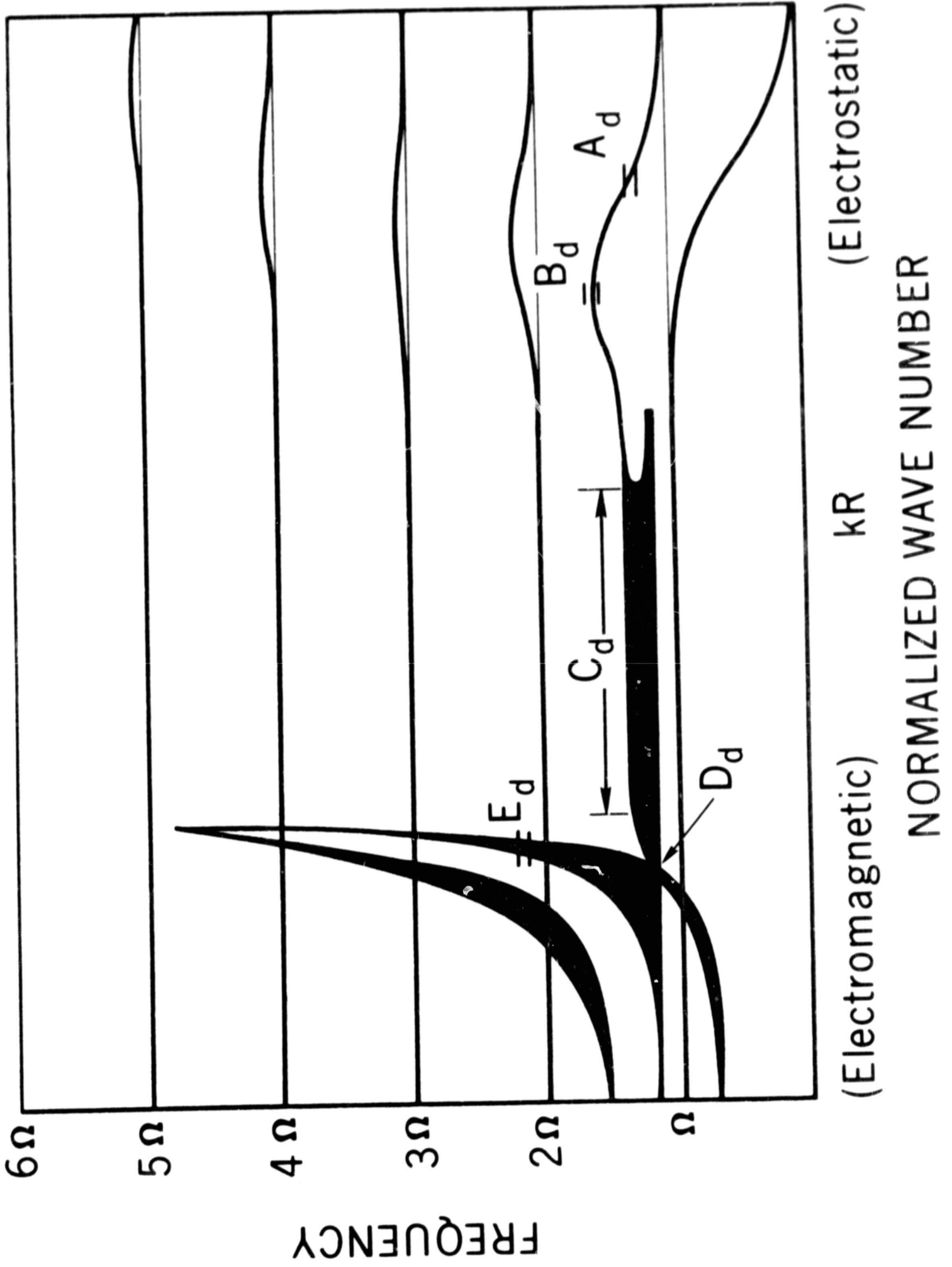


Figure 7

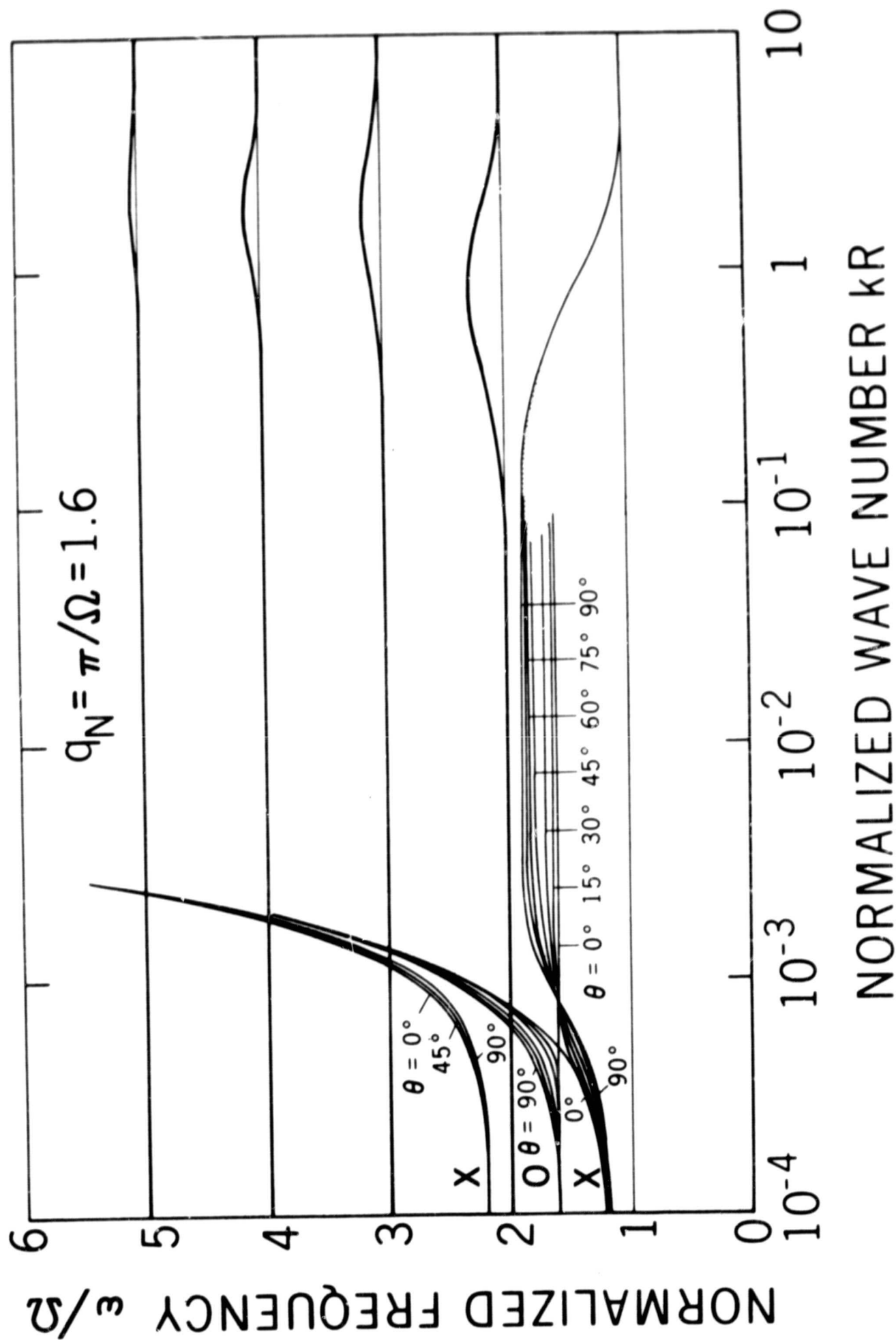


Figure 8

